Tuning the metamagnetism of an antiferromagnetic metal

J. B. Staunton,[1] M. dos Santos Dias,[1,2] J. Peace,[1] Z. Gercsi,[3] and K. G. Sandeman[3]

[1]*Department of Physics, University of Warwick, Coventry CV4 7AL, U.K.*

[2]*Peter Grünberg Institut and Institute for Advanced Simulation, Forschungszentrum Jülich and JARA, D-52425 Jülich, Germany*

[3]*Department of Physics, Blackett Laboratory, Imperial College London, SW7 2AZ, U.K.*

(Dated: February 4, 2013)

Abstract

We describe a 'disordered local moment' (DLM) first-principles electronic structure theory which demonstrates that tricritical metamagnetism can arise in an antiferromagnetic metal due to the dependence of local moment interactions on the magnetisation state. Itinerant electrons can therefore play a defining role in metamagnetism in the absence of large magnetic anisotropy. Our model is used to accurately predict the temperature dependence of the metamagnetic critical fields in CoMnSi-based alloys, explaining the sensitivity of metamagnetism to Mn-Mn separations and compositional variations found previously. We thus provide a finite-temperature framework for modelling and predicting new metamagnets of interest in applications such as magnetic cooling.

PACS numbers: 75.30.Kz, 75.10.Lp,75.50.Ee,75.30.Sg,75.80.+q

The application of a magnetic field to an antiferromagnet can cause abrupt changes to its magnetic state[1]. While such metamagnetic transitions have been known for a long time in materials such as $FeCl_2$[2] and MnF_2[3], it is their association with technologies like magnetic cooling[4] that has driven recent efforts to control metamagnetism in the room temperature range, and in accessible magnetic fields. Indeed a large, or even 'giant' magnetocaloric effect can arise at a first order metamagnetic phase transition such as is found in FeRh[5]. However, the thermomagnetic hysteresis associated with most first order transitions results in significant inefficiency during magnetic cycling. Therefore, (tri)critical transitions that straddle first order and second order behavior are of great interest. It is worth noting that tricritical points have also been examined in the context of other technologies, such as liquid crystal displays[6].

Given the interest in finding room temperature magnetic refrigerants, a re-examination of tricritical antiferromagnetic (AFM) metamagnets is warranted. At present there are only two first order magnetic refrigerants, La-Fe-Si[7] and MnFe(P,As,Si)[8] at an advanced stage of deployment in prototype cooling devices. Both materials are ferromagnets (FM) with field-induced metamagnetic critical points. However, tricriticality allows AFMs to emulate the low hysteresis, high entropy change properties of their FM cousins. For such real materials the greatest challenge is to understand the mixed localised/itinerant electron spin nature of their magnetism, and how this influences tricritical properties. Metamagnetic transitions, however, have previously been investigated in terms of either spin effect alone.

In AFM insulators[6], magnetic field-driven phase transitions can be understood qualitatively using a localised (classical) spin Hamiltonian with pairwise isotropic exchange interactions, a source of magnetic anisotropy and a Zeeman external magnetic field term. For example, Nagamiya[9] showed that, if the localised spins of a helical AFM are pinned by anisotropy and crystal field effects to spiral around a particular direction, the effect of a magnetic field brings about a first order transition to a fan structure where the moments now oscillate about the field direction. At higher fields, the fan angle smoothly reduces to zero to establish a high magnetisation phase at a second order transition. However, if anisotropy effects are negligible, the helical order has no favored axis and, once a magnetic field is applied, the helix plane orients perpendicular to the field. With increasing field the moments cant smoothly into a conical spiral towards the field's direction with a second order transition to a high magnetisation phase. Thus in this localised picture, first order

metamagnetism relies on a source of anisotropy.

Metamagnetism is accounted for differently in an itinerant electron system. Seminal work by Wohlfarth and Rhodes[10], Moriya and Usami[11], developed and extended by many others, e.g.[12,13], derived the coefficients of a Landau-Ginzburg free energy expansion for an AFM exposed to a uniform magnetic field in terms of the order parameter, $\Delta m_{\vec{q}}$, with wave-vector modulation $\vec{q}$. They considered both Stoner particle-hole excitations[10] and spin fluctuations[11,13] generated from the collective behavior of the interacting electrons[11,14,15]. Field-induced tricriticality occurs when the quadratic and quartic terms in $\Delta m_{\vec{q}}$ both equal zero. More recently, by analysing a generic mean-field Hamiltonian describing a helical state in an applied field Vareogiannis[16] has shown how an itinerant electron system can undergo a first-order 'spin-flip' transition. The AFM polarization is parallel to a weak applied field and flips perpendicular only if the field exceeds a critical value[17].

In this Letter we describe an ab-initio spin density functional theory (SDFT)-based 'local moment' theory for AFM to suit real materials where both itinerant and local spin effects are at play. Slowly varying 'local moments' can be identified from the complexity of the electronic behavior. We find that where magnetic anisotropy effects are small or neglected entirely, the local moments' AFM order can still undergo a first order transition to a fan or FM state owing to the feedback between the local moment and itinerant aspects of the electronic structure. We test our theory against a detailed experimental case study of CoMnSi-based tricritical metamagnets and show how it provides quantitative materials-specific guidance for tuning metamagnetic and associated technological properties.

A generalisation of SDFT[18] describes the 'local moment' picture of metallic magnets at finite temperature[19–22]. Its basic premise is a timescale separation between fast and slow electronic degrees of freedom so that 'local moments' are set up with slowly varying orientations, $\{\hat{e}_i\}$. The existence of these 'disordered local moments' (DLM) is established by the fast electronic motions and likewise their presence affects these motions. Moreover the local moments' interactions depend on the type and extent of the long range magnetic order through the associated itinerant electronic structure. The DLM picture of the paramagnetic state maps to an Ising picture[18] with, on average, one half of the moments oriented one way and the rest antiparallel. However once the symmetry is broken so that there is a finite order parameter $\{\vec{m}_i\}$ profile, e.g in a FM or AFM state and/or when an external magnetic field is applied, this simplicity is lost. Ensemble averages over the full range of non-collinear local

moment orientational configurations, $\{\hat{e}_i\}$, are needed to determine the system's magnetic properties realistically [22].

We now develop the DLM theory for a magnetic material in an external magnetic field $\vec{B}$ at a temperature T. The probability that the system's local moments are configured according to $\{\hat{e}_i\}$ is $P_i(\{\hat{e}_i\}) = \exp[-\beta\Omega(\{\hat{e}_i\},\vec{B})]/Z$ where the partition function $Z = \prod_j \int d\hat{e}_j \exp[-\beta\Omega(\{\hat{e}_i\},\vec{B})]$, $\beta = (k_B T)^{-1}$ and the free energy $F = -k_B T \ln Z$. A 'generalised' electronic grand potential $\Omega(\{\hat{e}_i\},\vec{B})$ is in principle available from SDFT[18] where the spin density is constrained to be orientated according to the local moment configuration $\{\hat{e}_i\}$. It thus plays the role of a local moment Hamiltonian but its genesis can give it a complicated form. Nonetheless by expanding about a suitable reference 'spin' Hamiltonian $\Omega_0\{\hat{e}_i\} = \sum_i \vec{h}_i \cdot \hat{e}_i$ and, using the Feynman Inequality[23], we find a mean field theoretical estimate of the free energy[18]

$$\begin{aligned} F(\{\vec{m}_i\},\vec{B},T) &= \langle\Omega(\{\hat{e}_i\},\vec{B})\rangle_{\{\vec{m}_i\}} \\ +k_B T \sum_i \int P_i(\hat{e}_i)\ln P_i(\hat{e}_i) d\hat{e}_i &- \vec{B}\cdot\sum_i \mu_i \vec{m}_i \end{aligned} \tag{1}$$

where $P_i(\hat{e}_i) = \exp[-\beta\vec{h}_i\cdot\hat{e}_i]/\int \exp[-\beta\vec{h}\cdot\hat{e}_i]d\hat{e}_i$, so that the set of local order parameters, $\{\vec{m}_i\} = \{\int \hat{e}_i P_i(\hat{e}_i) d\hat{e}_i\} = \{\langle\hat{e}_i\rangle\}$, each of which can take values between 0 and 1. This DLM self-consistent mean-field theory of the statistical mechanics of the local moments can be seen as the natural counterpart of the DFT self-consistent description of the interacting electrons. The first term of Eq. 1 is the local moments' internal energy, i.e. the average of the electronic grand potential over local moment configurations consistent with the order parameter profile $\{\vec{m}_i\}$, the second is $(-T)$ multiplied by the local moments' entropy and the last their interaction with a field, $\vec{B}$. The sizes of the local moments, $\{\mu_i\}$, are determined self-consistently[18] via the generalised SDFT.

The Weiss field at a site l is given by

$$\vec{h}_l = -\frac{\partial\langle\Omega(\{\hat{e}_i\},\vec{B})\rangle_{\{\vec{m}_i\}}}{\partial\vec{m}_l}. \tag{2}$$

To capture the itinerant electronic component of the problem coming from the overall spin-polarisation of the electronic structure, we approximate the $\vec{h}_l$ via an expansion about a

uniform $\vec{m} = \frac{1}{N}\sum_i \vec{m}_i$, i.e.

$$\vec{h}_l \approx -\left.\frac{\partial\langle\Omega\rangle}{\partial\vec{m}_l}\right|_{\vec{m}} - \sum_j \left.\frac{\partial^2\langle\Omega\rangle}{\partial\vec{m}_l\partial\vec{m}_j}\right|_{\vec{m}} \cdot (\vec{m}_j - \vec{m}) \qquad (3)$$
$$= \vec{h}(\vec{m}) + \sum_j \tilde{S}^{(2)}_{l,j}(\vec{m}) \cdot (\vec{m}_j - \vec{m}).$$

$\tilde{S}^{(2)}_{i,j}(\vec{m})$ is the direct correlation function and crucially describes effective interactions between the local moments that depend on the magnitude of $\vec{m}$. A solution of Eqs.1 to 3 at a fixed T and applied field $\vec{B}$ minimises the free energy F, Eq. 1. Several solutions, $\{\vec{m}^{(1)}_l\}$,$\{\vec{m}^{(2)}_l\}$,$\cdots$ may be found and the one with the lowest F describes the system's equilibrium state, $\{\vec{m}_l\}_{Equil.}$. Hence metamagnetic transitions can be tracked as functions of T and $\vec{B}$ - for a given T the solutions for increasing values of B can show a transition from, say, an AFM to a high magnetisation state at a critical field, B_c (e.g. see Fig. 1(b)). The material's spin-polarised electronic structure also depends on B and T and the state of magnetic order.

In order to elucidate the main aspects of the general framework laid out in Eqs.1 to 3 for a putative helical metal we assume temporarily that magnetic anisotropy effects are small and can be neglected. Without a magnetic field, $\vec{B}$, the solution $\{\vec{m}_l\}$ which produces the lowest free energy is $\vec{m}_i = \Delta m_{\vec{q}}(\cos(\vec{q}\cdot\vec{R}_i)\hat{x} + \sin(\vec{q}\cdot\vec{R}_i)\hat{y})$. The helical axis, $\hat{z}$, has no preferred direction in the crystal lattice. The order parameter $\Delta m_{\vec{q}}$ increases from 0 to 1 as T drops from T_N to 0 K. On applying $\vec{B}$, defining, say, the x-axis of our coordinate frame, we find numerical solutions of the mean field equations 1 to 3 of (i) distorted helical form: $\vec{m}_i = (m + \Delta m_{\vec{q}})\cos(\vec{q}\cdot\vec{R}_i)\hat{x} + \Delta m_{\vec{q}}\sin(\vec{q}\cdot\vec{R}_i)\hat{y}$, (ii) a conical helix: $\vec{m}_i = m\hat{x} + \Delta m_{\vec{q}}(\cos(\vec{q}\cdot\vec{R}_i)\hat{y} + \sin(\vec{q}\cdot\vec{R}_i)\hat{z})$, (iii) a fan state: $\vec{m}_i = m\hat{x} + \Delta m_{\vec{q}}\cos(\vec{q}\cdot\vec{R}_i)\hat{y}$ and (iv) a high magnetisation state with $\Delta m_{\vec{q}} = 0$. The free energies, functions of m, $\Delta m_{\vec{q}}$, $\vec{B}$ and T, are F_{dh}, F_{ch}, F_{fan} and F_{FM} respectively and we search for the lowest one at a given $\vec{B}$ and T. Consequently the relative difference between F_{dh} and any of the others determines whether there is a first order metamagnetic transition or not and also the T-dependence of the critical field, $\vec{B}_c$.

The local moment interactions $\tilde{S}^{(2)}_{i,j}(\vec{m})$ of Eq. 3 set up the Weiss field and, along with the uniform component, $\vec{h}(\vec{m})$[22], are the key elements of our theory. We determine these quantities using relativistic, spin-polarised, multiple scattering (Korringa-Kohn-Rostoker, KKR) theory and the coherent potential approximation (CPA)[22,24,25]. For the first time,

we account for the variation of $\tilde{S}^{(2)}_{i,j}(\vec{m})$ with increasing $\vec{m}$ driven by spin-polarisation of the itinerant electrons mediating the local moments' interactions[26,27]. Technical details on the calculations are found in the supplementary information[28].

Our previous experimental investigations revealed a class of magnetic materials based on the orthorhombic CoMnSi metal to be an ideal testing ground for the theory[31,32]. Those extensive magnetic and structural studies considered both the composition-dependent metamagnetism and pronounced magneto-elasticity in CoMnSi including a characterisation of the anomalous temperature variation of structural parameters in zero magnetic field. CoMnSi orders into an non-collinear, helical AFM state in zero magnetic field at $T_N \approx$380 K. In an applied field, $\vec{B}$, this transition becomes a metamagnetic one to a high magnetisation state at T_t. As B is increased T_t decreases before going through a tricritical point at around 2 Tesla where enhanced magnetocaloric and magnetostructural effects are observed. Typical of many useful magnetic metals, CoMnSi has magnetism with both localised and itinerant electron spin attributes[17]. Localised magnetic moments are identified with the Mn sites whereas the magnetism associated with the Co sites is reflected in the long range spin polarisation of the electronic structure. Our measurements found that the magnetism of CoMnSi is dominated by the behavior of the Mn moments. Their interactions, however, are delicately poised depending on the spacing between them[33] and their compositional environment.

We start with DFT-DLM calculations[34–36] for the paramagnetic ($m = 0$) state of CoMnSi. Local moments of magnitude $\mu \approx 3.0\mu_B$ establish on the Mn sites which are very close to the magnetisation per Mn site we, and another study[37], found in calculations of CoMnSi in a FM state ($m = 1$) showing that the Mn local moments' sizes are rather insensitive to the orientations of moments surrounding them. We thus use the 'frozen potential' approximation[24,38] to study CoMnSi for $\{P_i(\hat{e}_i)\}$ producing magnetic order parameters $\vec{m}_i$, each ranging between 0 and 1. For a finite long range order parameter, $m \neq 0$, we consider a probability distribution on a fine grid of local moment orientations [22,24]. No local moment forms on the cobalt sites in the DLM paramagnetic state (nor in our model of a commensurate approximation to the helical AFM state[31] found in experiment) whereas for finite m, a small magnetisation associated with each Co site is induced by the Mn moments lining up and the consequent overall spin polarisation of the electronic structure. For the FM state, $m = 1$, this is $\approx 0.6\mu_B$ per Co site[31,37]. The onset of magnetic order is found from examining $\tilde{S}^{(2)}_{i,j}(\vec{m})$ for the paramagnetic state, $m = 0$. By calculating the lattice Fourier

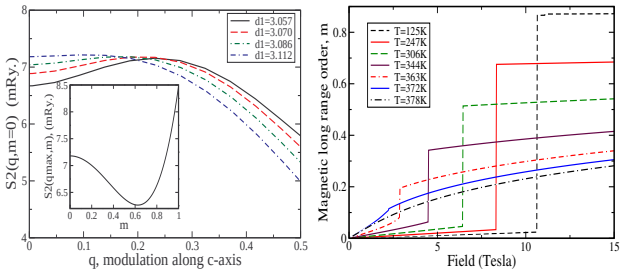

FIG. 1. (a) The Mn local moment interactions, $S^{(2)}(\vec{q},\vec{m}=0)$, for CoMnSi with structures measured in neutron diffraction experiments labelled by the Mn-Mn spacing, d_1, in Å. The inset shows $S^{(2)}(\vec{q}_{max},\vec{m})$ versus order parameter m for $d_1 = 3.07$ Å. (b) m versus applied field for several temperatures for a fixed lattice structure, in which $d_1 = 3.07$ Å. A tricritical point is indicated at 372 K, 2 Tesla.

transform, $\tilde{S}^{(2)}(\vec{q},0)$, and finding the wave-vector, $\vec{q}_{max}$, where it is greatest, we find the magnetically ordered state that the system forms below our mean-field theory estimate of $T_N = S^{(2)}(\vec{q}_{max},0)/3k_B$. If $q_{max} = 0$ a FM state is indicated whereas $q_{max} \neq 0$ indicates an AFM state. Fig.1(a) shows $S^{(2)}(\vec{q},0)$ using our structural data from neutron diffraction[31] which show the Mn-Mn distances, d_1, to vary by more than 2% over the temperature range 100-400K. Our calculations show that CoMnSi should order into an incommensurate helical AFM state along the c-axis, set by the orthorhombic crystal structure, at $T_N \approx 400$K in good agreement with experiment[31,32]. Since our calculations include spin-orbit coupling effects we checked that magnetic anisotropy effects are indeed small for this material (see[28]) as seen in measurement[39].

CoMnSi is near a FM instability as shown by the values of $S^{(2)}(\vec{q},0)$ in Fig.1(a) at $\vec{q}=0$ and $\vec{q}_{max}$ differing only slightly, a convenient signature for a potentially useful metamagnet. The tendency to order ferromagnetically takes over from the incommensurate ordering propensity as d_1 is increased, which experiment also shows to happen with increasing temperature. When the bath of electrons in which the Mn local moments sit becomes spin polarised as a magnetic field is applied and m increases, we find that the magnetic interactions, $\tilde{S}^{(2)}(\vec{q},\vec{m})$, weaken significantly as shown by the example of the inset to Fig. 1(a)[28]. This weakening promotes the stability of the distorted helical state over the others when the magnetic field is applied[37]. There can therefore be a first order transition to a fan, conical helix or high magnetisation state at critical field B_c despite the absence of magnetic

anisotropy. Fig. 1(b) illustrates this effect, and shows our solutions of the mean field theory equations 1 to 3 for one example. We point out that there are no adjustable parameters for these curves which show a transition from a distorted helical state (small m, B) to a high magnetisation state above a critical field B_c. The transition is first order up to a tricritical temperature of 372 K and second order thereafter.

Fig.2 shows the effect on $B_c(T)$ of either changing Mn nearest-neighbor separations, d_1, (Fig. 2(a)) or varying composition slightly away from CoMnSi (Fig. 2(b)). Tricritical points are denoted by asterisks. If the itinerant electron effect which gives $\tilde{S}^{(2)}(\vec{q},\vec{m})$ its $\vec{m}$-dependence is neglected and only the effects of a weak on-site magnetocrystalline anisotropy are included[28], we find the values of B_c to be 2 orders of magnitude smaller. B_c increases sharply as d_1 decreases, in line with measured pressure dependence of B_c of CoMnSi[40], and is very sensitive to compositional doping - the AFM tendency strengthens as electrons are removed ($CoMn_{0.95}Cr_{0.05}Si$) so that B_c increases, whereas it weakens when electrons are added ($Co_{0.95}Ni_{0.05}MnSi$).

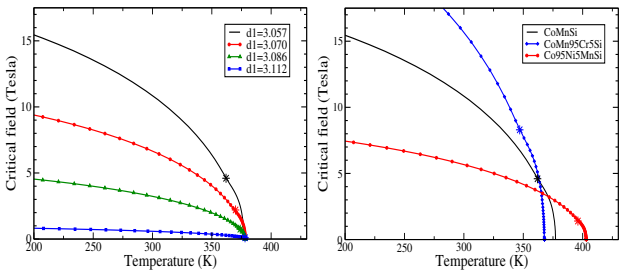

FIG. 2. (a) The critical field B_c for transition between a helical AFM and a high magnetisation state versus T for CoMnSi for the four structures used in Fig.1 and (b) for $Co_{0.95}Ni_{0.05}MnSi$, and $CoMn_{0.95}Cr_{0.05}Si$, with $d_1 = 3.057$ Å, (tricritical points denoted by asterisks).

To test the theory presented here we have used structural data taken in zero magnetic field[32] to predict the T-dependence of B_c in three CoMnSi-based compounds, comparing our findings with the experimental magnetic phase diagram extracted from magnetisation isotherms[32]. The lower panel, Fig. 3(b) shows our theoretical estimates of the critical fields. The magnitudes and trends are given very well by the theory. The increase of Mn-Mn separation d_1 with temperature is responsible for the concave appearance of $B_c(T)$ in CoMnSi. The use of correct structural data is very important to model the Ni-doped material. If we

instead use CoMnSi data to model this compound, we find much higher $B_c(T)$ values. This material is closer to ferromagnetism, as observed experimentally[32].

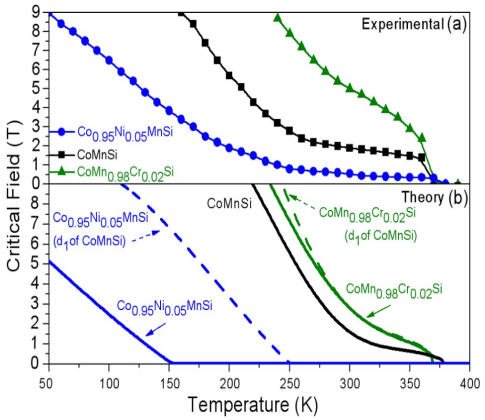

FIG. 3. (a) Experimental $B_c(T)$ for CoMnSi, $Co_{0.95}Ni_{0.05}MnSi$ and $CoMn_{0.98}Cr_{0.02}Si$[32].(b) Theoretical $B_c(T)$ for the same three systems, modelled using the lattice parameters found from neutron diffraction[32] in zero field. The $B_c(T)$ of the Ni- and Cr-doped systems modelled using the CoMnSi structural data is also shown (dashed lines) to highlight the relative importance of accurate structural data.

Detailed theoretical models are needed to use in concert with experimental studies if the behavior of highly sensitive magnetic materials is to be analysed and tuned. We have discussed one such model here and showed how the temperature and field dependence of the metamagnetic transition of an antiferromagnetic metal can be affected by varying composition and atomic spacing. Useful magnetic metals typically have large magnetic moments which are established locally. The Disordered Local Moment model works well for these[22,29,30] and we have set out a theory for metamagnetic transitions based on this picture. An important aspect for magnetic material design is to distinguish first and second order magnetic transitions and to get some control of the location of precious tricritical points. Our CoMnSi case study reveals how decreasing the Mn-Mn separation, d_1, or reducing the number of electrons by compositional doping increases the critical field. One notable feature in our modelling is the dependence of the interaction between the local moments upon the extent of long range magnetic order. This comes from the change in the behavior of the itinerant electrons that mediate these interactions and produces a mechanism for first-order

'spin-flip' transitions even for cases where there is little magnetic anisotropy. This aspect has an important role in the analysis and design of adaptive, magnetic metals.

We acknowledge financial support from the EPSRC (UK) (J.B.S, J.P), a FCT Portugal PhD grant SFRH/ BD/35738/2007 (M.d-S.D), the Royal Society (K.G.S) and EPSRC grants EP/G060940/1 and EP/E016243/1 (Z.G). K.G.S. thanks M. Avdeev and J. Bechhöfer for useful discussions.

---

[1] E. Stryjewski and N. Giordano, Adv. Phys. **26** 487 (1977).

[2] I. S. Jacobs and P. E. Lawrence, Phys. Rev. **164** 866 (1967).

[3] I. S. Jacobs and P. E. Lawrence, J. Appl. Phys. **35** 996 (1964).

[4] K.G. Sandeman, Scripta Materialia **67**, 566, (2012).

[5] M.P. Annaorazov et al., Cryogenics **32** 867 (1992).

[6] P. M. Chaikin and T. C. Lubensky, *Principles of condensed matter physics*, C.U.P. (2000).

[7] J. Liu et al., Scripta Materialia **67**, 584, (2012).

[8] N.H. Dung et al., Adv. Energy Mater. 1, 1215 (2011).

[9] T. Nagamiya et al., Prog. Theor. Phys. **27**, 1253, (1962).

[10] E. P. Wohlfarth and P. Rhodes, Phil. Mag. **7**, 1817, (1962).

[11] T. Moriya and K. Usami, Sol. Stat. Comm. **23**, 935, (1977).

[12] M. Shimuzu, J. Physique **43**, 155, (1982).

[13] H. Yamada and T. Goto, Phys. Rev. B **68**, 184417, (2003).

[14] *Electron Correlations and Magnetism in Narrow Band System*, edited by T. Moriya (Springer, N.Y., 1981).

[15] J. Kübler, *Theory of Itinerant Electron Magnetism*, Clarendon Press (2000).

[16] G. Varelogiannis, Phys.Rev.Lett. **91**, 117201, (2003).

[17] K. Irisawa et al., Phys. Rev. B **70**, 214405, (2004).

[18] B. L. Gyorffy et al. J. Phys. F **15** 1337,(1985).

[19] J. Hubbard, Phys. Rev.B **20**, 4584, (1979).

[20] H. Hasegawa, J. Phys. Soc. Japan **46** 1504, (1979).

[21] J. B. Staunton and B. L. Gyorffy, Phys.Rev.Lett. **69**, 371, (1992).

[22] J. B. Staunton et al., Phys.Rev.Lett. **93**, 257204, (2004).

[23] R. P. Feynman, Phys. Rev. **97**, 660, (1955).

[24] J. B. Staunton et al., Phys. Rev. B **74**, 144411, (2006).

[25] M. dos Santos Dias et al., Phys. Rev. B **83**, 054435 (2011).

[26] L. M. Sandratskii et al. Phys. Rev. B **76**, 184406, (2007).

[27] S. Polesya et al., Phys. Rev. B **82**, 214409, (2010).

[28] Online supplementary information:

[29] I. D. Hughes et al., Nature, **446**, 650, (2007).

[30] I. D. Hughes et al., New J. Physics, **10**, 063010, (2008).

[31] A. Barcza et al. Phys.Rev.Lett. 104, 247202, (2010).

[32] A. Barcza et al., arXiv:cond-mat/1208.3176.

[33] Z. Gercsi et al., Phys. Rev. B 83, 174403, (2011).

[34] G. M. Stocks et al., Phys. Rev. Lett. **41**, 339, (1978).

[35] D. D. Johnson et al., Phys. Rev. Lett. **56**, 2088, (1986).

[36] H. Ebert et al., Rep. Prog. Phys. **74**,096501, (2011).

[37] V. I. Valkov et al., Low Temp. Phys. **36**, 1064, (2010).

[38] J. Harris, Phys. Rev. B **31**, 1770, (1985).

[39] K. Morrison et al., Phys. Rev. B **78** 134418 (2008).

[40] Yu. D. Zavorotnev et al., J. Mag. Magn. Mat. **323**, 2808, (2011).